Breakdown characteristics in nonplanar geometries and hollow cathode pseudospark switches

Hoyoung Pak[a] and Mark J. Kushner[b]

University of Illinois, Department of Electrical and Computer Engineering, 1406 West Green Street, Urbana, Illinois 61801

Breakdown voltages of gases in parallel-plate geometries are well represented by Paschen's law, whose scaling parameter is *pd* (gas pressure×electrode separation). In nonplanar geometries, Paschen's law is not directly applicable due to the ambiguity in the distance between the electrodes and distortion of the electric field. A Monte Carlo computer model is used to investigate breakdown characteristics in nonplanar geometries and hollow cathode pseudospark switches in particular. The model tracks the trajectories of both electrons and ions, including ionizing collisions in the gas phase by electrons and ions, and secondary electron emission by ions on surfaces. It is found that under typical operating conditions in helium (0.1 to a few Torr, voltages of tens of kV, effective electrode separation of a few mm), approximately two-thirds of ionizing collisions are attributable to ion impact, of which half are due to ion impact in the gas phase.

I. INTRODUCTION

The breakdown of gases in parallel-plate geometries has been studied for many years,[1] and has resulted in a well-known characterization of the breakdown voltage called Paschen's law. This relationship states

$$V_b = F(pd), \tag{1}$$

where V_b is the breakdown voltage, p is the gas pressure, and d is the electrode separation. The generalized breakdown condition is obtained by determining the voltage, for a given pd, at which the generation of electrons by direct electron impact (e.g., ionization, detachment) and secondary processes (e.g., photoionization, ion impact on electrodes), and the losses of electrons (e.g., attachment) result in at least a self-sustaining current. In its simplest form, the current in a plane-parallel gap in a nonattaching gas is given by

$$I = I_0 \exp(\alpha d)/\{1 - (\omega/\alpha)[\exp(\alpha d) - 1]\}, \tag{2}$$

where α (cm^{-1}) is the first Townsend coefficient for ionization, and ω (cm^{-1}) is an effective secondary ionization coefficient. ω/α is the number of secondary electrons produced for every primary ionization in the gas phase. In most cases, α is a strong function of E/N (electric field/gas number density) while ω is a weak function of E/N. ω accounts for a number of secondary processes, including ion impact on the electrodes, photoionization, and ion impact in the gas phase. Breakdown is that voltage which satisfies

$$(\omega/\alpha)[\exp(\alpha d) - 1] = 1. \tag{3}$$

The dependence of V_b on pd at low values of pd for plane-parallel electrodes is shown in Fig. 1. Paschen's law specifies that a minimum breakdown voltage occurs at pd_0 of a

few Torr-cm. The increase in V_b at values of $pd < pd_0$ results from the decreasing likelihood of ionizing collisions caused by the decrease in the area density of gas. The increase in V_b at values of $pd > pd_0$ results from the requirement that one must have a critical value of E/N to achieve a self-sustaining current.

Departures from Paschen's law results from both nonequilibrium and geometrical effects. The formulation of Paschen's law requires that the ionization coefficient be a well-characterized function of E/N. If the electrons are not in equilibrium with the local value of E/N, then electron multiplication across the gap cannot be explicitly given by $\exp(\alpha d)$. A first-order correction for this effect is to express electron multiplication across the gap as $\exp[\alpha(d - d')]$ where d' is the distance required for electrons to drift before coming in equilibrium with the electric field.

Geometrical effects are primarily manifested by E/N being a function of position between the electrodes, as in cylindrical or point-to-plane structures. Assuming that the electron-energy distribution is in equilibrium with the local electric field (commonly called the local-field approximation), electron multiplication between the cathode and anode is given by

$$M = \int p(\mathbf{s}) \exp\left[\int_{\mathbf{r(s)}} \alpha\left(\frac{E(\mathbf{r})}{N}\right) dr \right] d\mathbf{s}, \tag{4}$$

where $p(\mathbf{s})$ is the probability for electron emission occurring at location $\mathbf{s}$ on the cathode and $\mathbf{r(s)}$ is the path followed by electrons from that location. In symmetric geometries, such as coaxial cylinders, $p(\mathbf{s})$ is a constant. In point-to-plane geometries, $p(\mathbf{s})$ is heavily weighted towards the high-field region near the point. Under conditions where the local-field approximation is not valid and geometrical effects are important, semianalytic expressions for V_b become increasingly less accurate.

In gases such as He and H_2, ion energies can reach many hundreds of eV for holdoff voltages of only a few kV.
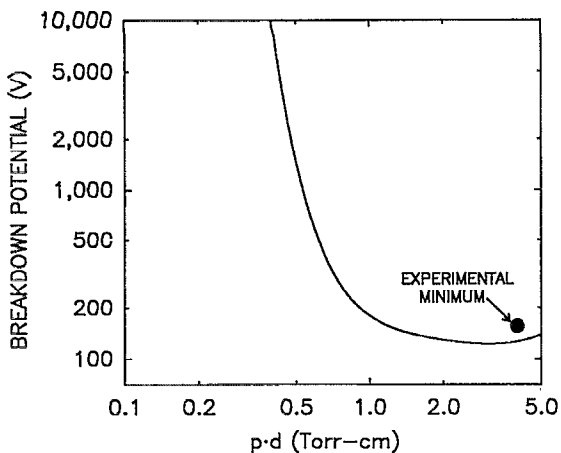

FIG. 1. Simulated Paschen curve for breakdown between parallel plates in He. The experimental minimum breakdown voltage is at $pd=4$ Torr cm (Ref. 10).
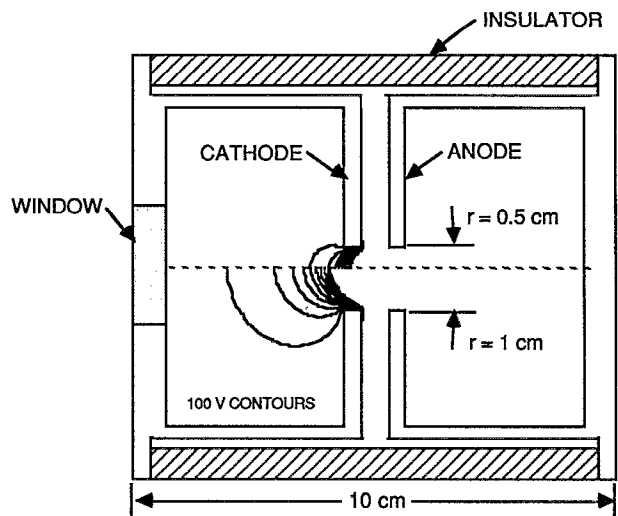

FIG. 2. Schematic of the optically triggered pseudospark switch which consists of an opposing cylindrical hollow cathode and anode with central holes. The device is triggered by uv illumination through the window and typically operates at gas pressures of <1 Torr. Two views are shown having cathode hole radii of 0.5 and 1 cm. Electric potential contours (0–1 kV, 100 V spacing) are shown for a holdoff voltage of 10 kV. More potential penetration into the cathode occurs with the larger hole.

In recent work by Phelps and Jelenkovic,[2] the importance of accounting for excitation and ionization by heavy particle impact (energetic ions and neutrals) was investigated at high E/N. They found that experimental observations of excited-state emission could not be explained on the basis of electron impact excitation alone, and was largely attributable to ion impact. In He, the cross section for ion impact ionization exceeds that for electron impact at energies >200 eV and increases for higher particle energies, while that for electrons decreases.[3] In conventional dc or pulsed discharges, this condition is of little consequence since ions have a low probability of being accelerated to those energies. During high-voltage holdoff in, for example, thyratrons, ions can exceed those energies, and therefore significantly contribute to ionization.

The relative rate of secondary electron emission from the cathode by ion bombardment, γ, is also a strong function of ion energy. γ is nearly constant at energies of less than a few hundred eV. However, γ normally increases with increasing energy, and can exceed unity for energies greater than many keV.[4,5] The rate of secondary electron emission by ion bombardment is also a sensitive function of the surface of the cathode. γ is typically smaller for clean surfaces, and larger for oxidized surfaces.

In this paper, we theoretically investigate the breakdown of gases in hollow cathode plasma switches where both geometrical and nonequilibrium effects are important. The particular switch of interest is the optically triggered pseudospark[6,7] which consists of an opposing hollow cathode and anode having central holes (see Fig. 2). The pseudospark has found application as both a particle beam generator and as a plasma switch. The optically triggered pseudospark has demonstrated high currents ($I > 30$ kA), high current densities ($I > 10^4$ A cm^{-2}), and high rates of current rise ($dI/dt > 10^{11}$ A s^{-1}). Its interesting properties include its compact size, thereby reducing inductance, and its ability to electrically float. Due to the nonplanar geometry of the pseudospark, Paschen's law is difficult to apply. This results both from the nonequilib-

rium nature of the electron transport and from the difficulty in defining an effective path length. Since pseudosparks operate on the "near side" of Paschen's curve (increasing V_b with decreasing pd), electrons having longer paths will decrease V_b due to their having more opportunity to avalanche before reaching the anode. Since the spatial distribution of the electric field, both in the gap and in the hollow electrode structures, depends on parameters such as the electrode separation, electrode thickness, and electrode hole radii, V_b will also depend on these quantities.

In conventional operation, hollow cathode pseudospark switches are triggered, either by a uv photon flux or electrically. The onset of avalanche and the rate of current rise are significantly affected by the distortion of the electric field in the hollow cathode by space charge.[8–11] In some cases the trigger charge is sufficiently large to distort the fields without additional multiplication. In this respect our study directly addresses the pretriggering holdoff phase of operation of switches, or switches that are triggered with, for example, low uv fluxes where space charge may not be important.

In Sec. II we describe our model for holdoff in nonplanar geometries followed by a discussion of our results in Sec. III. Our concluding remarks are made in Sec. IV.

II. DESCRIPTION OF THE MODEL

Many models of hollow cathode pseudospark switches have recently been published whose goals are to address the nonequilibrium plasma transport during commutation and conduction.[8–11] The models have incorporated drift diffusion,[9,10] Monte Carlo-fluid,[8] and multielectron group methods.[11] In each case, though, an initial electron density

was assumed or the device was externally triggered. The breakdown, or holdoff, capabilities of the switch were not addressed. The model we have used in this study of breakdown in pseudosparks is a three-dimensional Monte Carlo simulation. Since the sources of ionization in high-voltage devices depend on the energy distributions of both electron and ions, the trajectories of both of these species are accounted for in the model. The decision to include ions as pseudoparticles in the model was also made based on observations that the cathode near the central hole melts during the current pulse. An analysis of the power flux of particles to the surface during commutation that is required for the surface to melt[7] implies that the ions must have energies substantially greater than their equilibrium values based on the local E/N. He is used as the gas in this study, a choice based on the observation that He has superior holdoff abilities compared to H_2 under many conditions.[12] The geometry used in this study is that of the optically triggered pseudospark,[6] and is shown in Fig. 2. The dimensions and thickness of all of the electrode structures, as well as their surface properties, can be specified in the model.

The simulation begins by calculating the electric field by solving Laplace's equation. Since during the breakdown stage deformation of the electric field by space charge is minimal, the vacuum fields are used in this study. Laplace's equation is solved using the method of successive over relaxation. The numerical mesh used for this purpose is nonuniform, with a higher density of mesh points in the gap and in the high-field regions.

The mechanics of the Monte Carlo simulation will be briefly discussed. The trajectories of the electron and ion particles are advanced for a time Δt based on a number of criteria. The time step is chosen to be the smaller time required to travel a distance over which the electric changes by a specified amount and the time to the next collision. The null collision method[13] is used to select the time between collisions. This method is used because a particle's energy can change from thermal values to many keV between collisions and there is a commensurate change in the particle's collision frequency. This makes the initial choice of collision time ambiguous. In the null collision method, a fictitious cross section is added to the real cross section at every energy so that the total collision frequency appears to be a constant. With this condition the time to the next collision is given by

$$\Delta t = -(1/\nu_t)\ln(r), \qquad (5)$$

where ν_t is the total collision frequency including the null contribution and r is a random number evenly distributed on (0,1). At the time of the collision, a second random number r is chosen. If $r < \nu(\epsilon)/\nu_t$, where $\nu(\epsilon)$ is the actual collision frequency at the current energy, then a collision occurs. If the inequality does not hold, the collision is said to be null, and the particle proceeds unhindered.

In case of a real collision, another random number is used to determine the type of collision. If the collision is an ionization by an electron, a secondary electron is placed at

the site of the ionization. The energy of the secondary electron is given by an extrapolation of the data of Opal, Peterson, and Beatty.[14] For an ionizing collision by an ion, the secondary electron is assumed to have only thermal energy. The energy of the primary particle is reduced by the inelastic energy loss and is anisotropically scattered. The scattering angle for electrons is energy dependent, being isotropic at low energies and becoming forward scattered at higher energies. In ion charge-exchange collisions, the energy of the new ion is assumed to be thermal with an isotropic trajectory. In ion impact collisions resulting in an ionization, the scattering of the ion is assumed to be forward.

The flow of the computer model is as follows. A preselected number of electrons having an average energy of a few eV are uniformly released from the cathode surface facing the anode, in the hole, and along the back side of the cathode. Electrons are then transported in the electric field while the number and location of ionizing collisions are recorded. The next step is to transport ions, with an ion being started at the location of each of the previous ionizations by electrons. The location of the heavy particle ionizing collisions are similarly recorded. When an ion strikes the cathode, an appropriate number of electrons are released as specified by the secondary electron emission coefficient. The transport of ions progresses until all ions are collected. Any electrons previously generated by ion impact are then transported. At this point, the first "wave" of particle transport has been completed. Breakdown is said to occur if the number of electrons generated by electron and ion impact (and collected by the anode) compared to the initial number released exponentially increases. If breakdown does not occur, or better statistics are required, additional "waves" of electrons can be released. Since this calculation does not directly address the time development of the electron swarm, this criterion for breakdown is only strictly applicable to conditions where there is a quasi-steady-state source of electrons on the cathode due, for example, to field emission. Since the transit time for both electrons and ions is less than tens to hundreds of ns, these breakdown criteria may also be applied to switches that are pulse charged in a few microseconds.

Cross sections for electron impact processes were obtained from Refs. 15–17. Cross sections for ion impact processes in the gas phase were obtained from the compilation of Janev et al.[3] Secondary emission coefficients as a function of ion energy for the Mo cathode were scaled from Refs. 4 and 5.

III. BREAKDOWN CHARACTERISTICS

A. Breakdown voltages

To validate our model, we simulated breakdown voltages for plane-parallel geometries. Our predicted breakdown voltages as a function of pd are shown in Fig. 1. The minimum potential at which breakdown occurs V_{min} is approximately 150 V which corresponds to $E/N = 1.2 \times 10^{-15}$ V cm^2 and $pd_0 = 4.0$ Torr cm. The precise value of pd_0 and V_{min} depend on the secondary electron
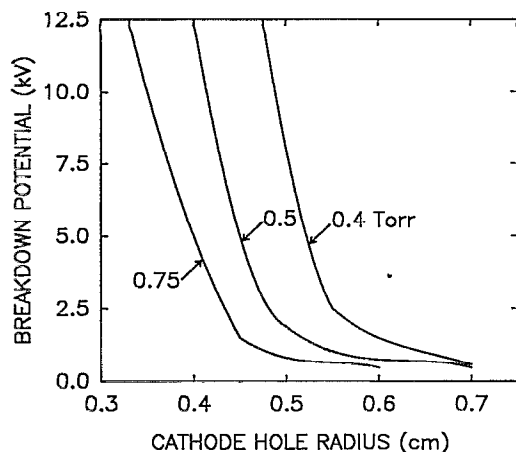
H. Pak and M. J. Kushner   96

FIG. 3. Breakdown voltage as a function of cathode hole radius for various He gas pressures. The electrode separation is 0.5 cm and the cathode thickness is 0.4 cm. Operating with large cathode holes effectively increases pd.
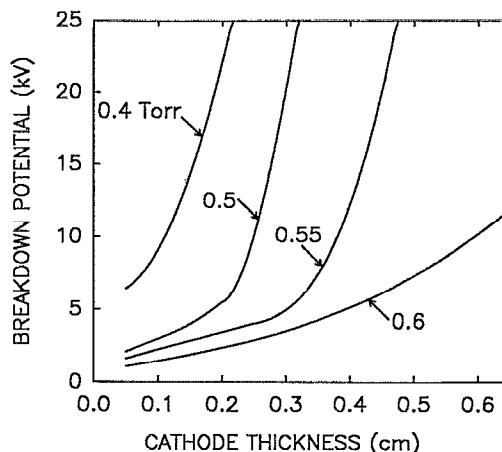

FIG. 4. Breakdown voltage as a function of cathode thickness for various He pressures. The electrode separation is 0.5 cm. Increasing the cathode thickness decreases potential penetration, and effectively decreases pd.

coefficient and state of the cathode. Given these dependencies our value agrees well with experiments.[10] On the left-hand side of the minimum, commonly known as the near side of Paschen's curve, the holdoff voltage increases with decreasing pd because of the increasing mean free path of electrons relative to the electrode separation. This results in a decreasing probability of ionizing collisions. At high gas pressures and large electrode separations, higher voltages are required to break down the gas because of the necessity to maintain a critical E/N.

As perturbations to the electric field are introduced due to nonplanar geometries, deviations from Paschen's law are expected. Using the geometry of the optically triggered pseudospark, the dependence of breakdown voltage on cathode hole radius is shown in Fig. 3 for various gas pressures. The electrode separation is 0.5 cm and the thickness of the cathode is 0.4 cm. For a given gas pressure, breakdown occurs above the curve while holdoff occurs below the curve. As the cathode hole radius increases, the holdoff voltage decreases due primarily to increased penetration of the anode potential through the cathode hole into the interior of the hollow cathode, as shown in Fig. 2. This increases the effective path length d through regions that have a high electric field. In this respect, increasing the radius of the cathode hole can be viewed as being equivalent to increasing the electrode separation of plane parallel-electrode geometries. The breakdown potential approaches $V_{\min}$ as the cathode hole radius increases because electron trajectories from the cathode have pd that approach and exceed 4 Torr cm in regions where $E/N \geqslant 1.2 \times 10^{-15}$ V cm². Electrons originating from the rear surface of the cathode facing the hole are unimportant since the E/N deep in the cathode is smaller than the critical value. For a given cathode hole radius, the holdoff voltage decreases with increasing pressure, commensurate with operating on the near side of Paschen's curve.

The dependence of V_b on the thickness of the cathode at various gas pressures is shown in Fig. 4. The electrode

separation is 0.5 cm and the radius of the electrode holes are 0.4 cm. V_b increases with increasing electrode thickness due to a reduction in the penetration of anode potential into the hollow cathode thereby effectively reducing pd. Smaller cathode hole radii or larger cathode thickness cause the breakdown relationship to more closely represent Paschen's law. For cathode thickness exceeding 0.5 cm, breakdown is caused by electron avalanche occurring at the front face of the cathode. For thicknesses less than this value, avalanche occurs dominantly adjacent to the cathode hole in the interior of the cathode, an indication of long path breakdown (see below.)

B. Electron impact ionization

The locations at which electron impact ionizations occur are shown in Fig. 5 for plane-parallel and hollow electrode geometries. The gas pressure is 0.5 Torr and the holdoff voltage is 10 kV. In the plane-parallel geometry, electron impact ionizations are randomly distributed as a function of radius, a consequence of their initial distribution being random across the face of the cathode. The locations of the ionizations are fairly close to the cathode within the gap. This latter point is a consequence of there being a maximum in the cross section for electron impact ionization of helium at 130 eV. Therefore, electrons are more likely to undergo ionizations when they have lower energies, which occurs near the cathode.

In hollow-cathode planar-anode structures, though, ionizations occur predominantly near the central hole by electrons initially emitted from the inside of the cathode. This behavior is a consequence of the electrons in the hollow cathode spending a longer time in the moderate electric fields resulting from potential penetration into the cathode. They also have a longer effective path length to the anode resulting in a large pd. In the hollow anode case, the majority of electron impact ionization occurs in the cathode hole and near gap. Once the electrons advect into the high-field region in the gap proper and accelerate to
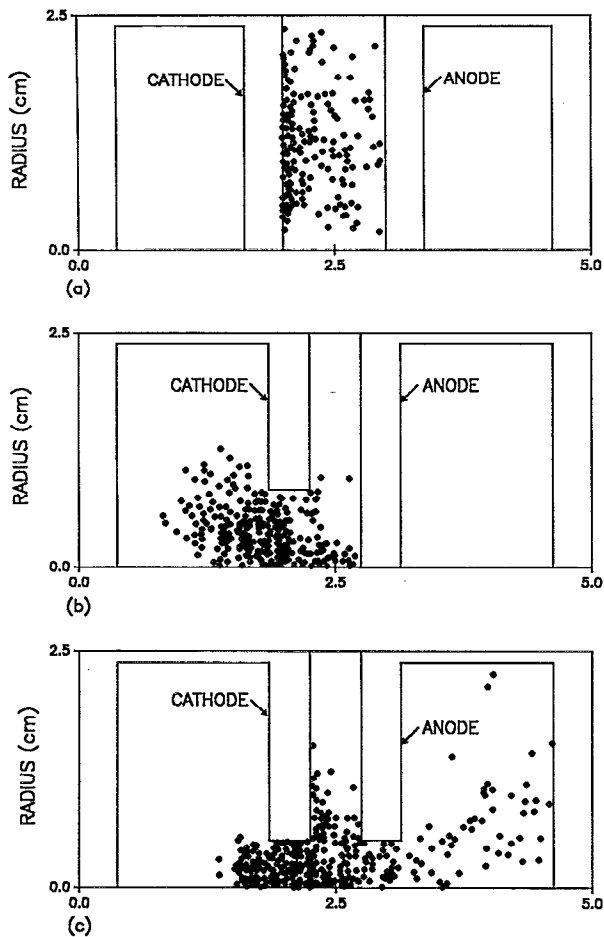
FIG. 5. Locations of electron impact ionization events for (a) plane-parallel, (b) hollow cathode and planar anode, and (c) hollow anode geometries. The He gas pressure is 0.5 Torr and holdoff voltage is 10 kV. The locations of electron impact ionization are primarily on the cathode side of the gap.
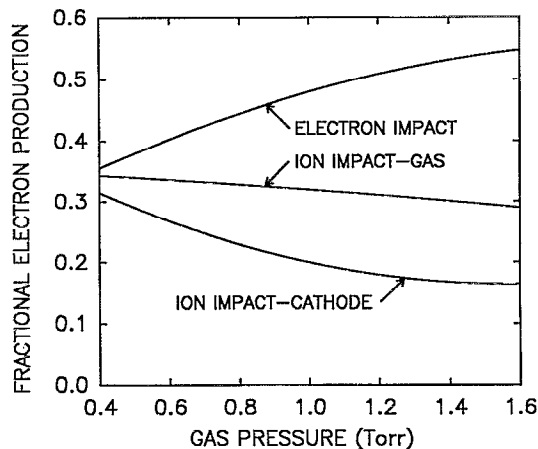

FIG. 6. Fractional contributions to electron production by electron impact, ion impact in the gas, and ion impact on the cathode for He with a holdoff voltage of 10 kV. For pressures below 1 Torr, the majority of electron production is due to ion impact processes.

energies greater than the peak in the ionization cross section, the rate of ionization decreases. The amount of ionization that occurs in the hollow anode is minimal, since electrons accelerated into the anode have energies of many hundreds of eV to keV and their effective mean free paths are many cm. Boeuf and Pitchford calculated locations of electron impact ionizations for the planar anode geometry and found substantially more ionizations occurring in the hole and gap during commutation.[8] In their work, the cathode hole radius was 2.8 mm and holdoff voltage 2 kV. The penetration of potential deep into the cathode is not as great for these conditions.

C. Ion impact ionization and ion energy distributions

The contribution of ion impact processes to ionization during holdoff can be substantial, and in some cases exceed that of electrons. The fractional contributions of electron impact, ion impact in the gas, and ion impact on surfaces are shown in Fig. 6 as a function of gas pressure. The holdoff voltage is 10 kV. At large values of V/p, the total contribution of ion impact to ionization is approximately

twice that by electron impact, with the contribution by ion impact in the gas phase and on the cathode being nearly equal. As the gas pressure increases, the fractional contribution from electron impact increases primarily at the expense of ion impact on the cathode. Under most conditions, the contribution by ion impact in the gas phase exceeds that by ion impact on surfaces.

These large contributions to ionization by ion impact are a consequence of the high ion energies that can be generated during holdoff. The distributions of ion energies striking the cathode for a pressure of 0.5 Torr and holdoff voltage of 10 kV are shown in Fig. 7 for hollow anode and planar anode geometries. The ion energy distribution is fairly broad, with a tail that extends to the full anode potential. The average ion energy striking the electrode is 630 eV for the planar anode. Substantial differences in the ion
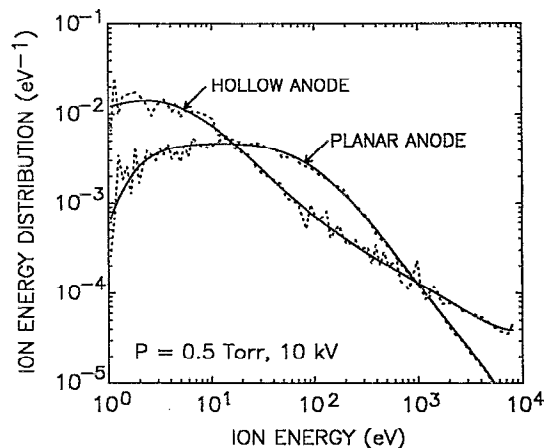

FIG. 7. Ion energy distributions striking the cathode for a holdoff voltage of 10 kV in 0.5 Torr He for hollow anode and planar anode geometries. The dotted line is raw data and the solid line is a polynomial fit. The average ion energy striking the cathode is 630 eV for the planar anode, with the maximum ion energy extending to the anode potential.
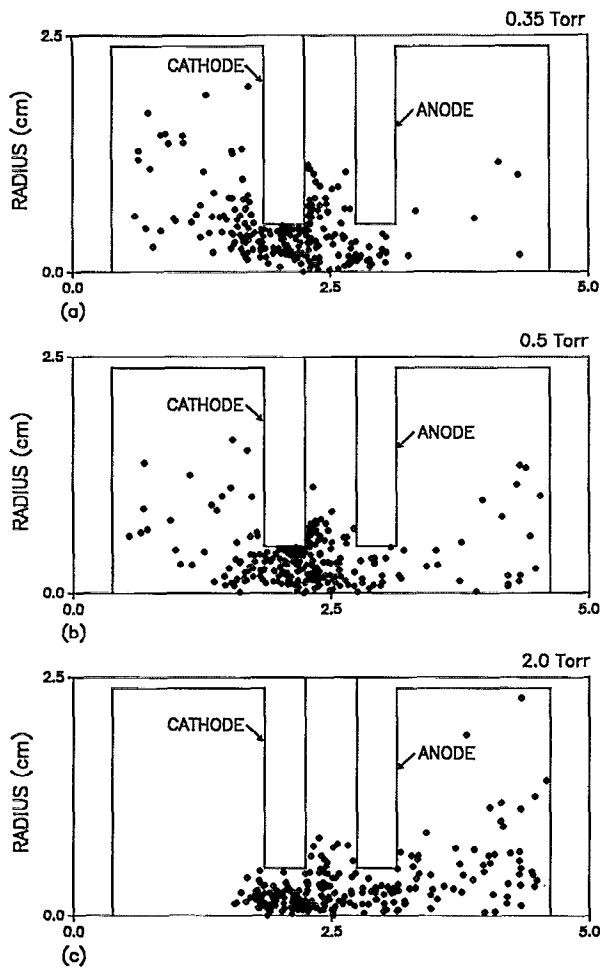
FIG. 8. Locations of ion impact ionization in the gas for pressures of 0.35, 0.5, and 2.0 Torr. The holdoff voltage is 10 kV.
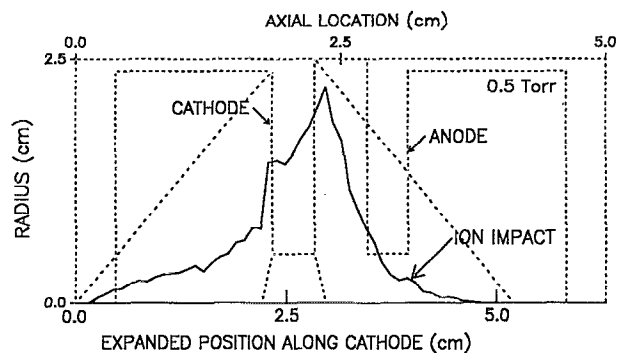

FIG. 9. Relative distribution of ions striking the cathode as a function of position. The dotted lines show the outline of the switch and the mapping of impact locations. The solid trace shows the relative frequency of ion impact.

energy distributions are found between the hollow anode and planar anode cases. In the hollow anode case, more ions are generated both near the cathode (in the cathode hole) and nearer the anode (see Fig. 5). This accounts for there being both a larger low-energy component and larger high-energy tail to the ion energy distribution.

The locations of ion impact ionization in the gas phase during holdoff for three different gas pressures are shown in Fig. 8. Ion impact ionizations preferentially occur near or deep inside the cathode at lower pressures since ion energies are highest at those locations. (Recall that the ion impact ionization cross section monotonically increases with energy for these conditions.) Electrons produced by ion impact deep in the cathode have a larger effective pd, and therefore generate more ionization leading to breakdown. At higher pressures less ionization by ion impact occurs in the cathode since ions cannot penetrate as far from the gap. More ion impact ionization occurs in the anode based largely on there being more ions generated there by electron impact at higher pressures.

The distribution of ion impact events on the cathode is shown in Fig. 9. The ions preferentially strike on the cathode lip nearest the anode where the maximum in electrode erosion is also observed.[6] The ions that strike this location originate deep inside the anode, and have the highest kinetic energy (hundreds of eV to keV). Ions formed in the gap preferentially strike the inner surface of the hole and hollow cathode, and have lower energies.

On very short time scales, that is less than the ion transit time, the contribution of ion impact phenomena to breakdown will be less than that described here. In that respect, one can expect higher breakdown voltages under pulse-charging conditions than described here. Many workers over the years have measured higher holdoff voltages for pulse charging than for dc charging, a phenomenon usually attributed to the statistical time lag required to generate seed charges for avalanche.[19] The formative time lag is that time required for the subsequent electron avalanche to close the switch, and accounts for transit time effects due to both electron impact processes and ion impact processes. Given the apparent importance of ion impact ionization, the improved holdoff obtained under pulsed conditions may, in part, be attributable to a reduction in the ion contribution to avalanche during the formative time lag.

IV. CONCLUDING REMARKS

A Monte Carlo model has been developed to study holdoff in nonplanar geometries, and in the hollow cathode pseudospark switch in particular. Deviations from Paschen's law resulting in lower holdoff voltages are caused by penetration of anode potential into the hollow cathode making a larger effective pd. Penetration increases with increasing cathode hold radius and decreasing cathode thickness, and so the holdoff voltage decreases. The contribution of ion impact to ionization is substantial, and can exceed that due to electron impact. The average energies of ions striking the cathode during holdoff and the beginning of commutation is many hundreds of eV, and have maximum values of nearly the anode potential. The contribution of ion impact ionization can be minimized by using heavier molecular weight gases, since the cross section for electron impact scales with the velocity of the ion which

decreases with increasing mass, and momentum transfer cross sections generally increase with increasing mass.

ACKNOWLEDGMENTS

[1] J. M. Meek and J. D. Craggs, *Electrical Breakdown of Gases* (Wiley, Norwich, 1978), and references therein.

[2] A. V. Phelps and B. M. Jelenkovic, Phys. Rev. A **38**, 2975 (1988).

[3] R. K. Janev, W. D. Langer, K. Evans, and D. E. Post, *Elementary Processes in Hydrogen-Helium Plasmas* (Springer, Berlin, 1987), Chaps. 2 and 5.

[4] B. Szapiro and J. J. Rocca, J. Appl. Phys. **65**, 3713 (1989).

[5] J. Ferrón, E. V. Alonso, R. A. Baragiola, and A. Oliva-Florio, J. Phys. D **14**, 1707 (1981).

[6] W. Hartmann and M. A. Gundersen, in *Physics of Pseudosparks*, edited by M. A. Gundersen and G. Schaefer (Plenum, New York, 1990), pp. 77–88, and references therein.

[7] W. Hartmann, V. Dominic, G. F. Kirkman, and M. A. Gundersen, J. Appl. Phys. **65**, 4388 (1989).

[8] J. P. Boeuf and L. C. Pitchford, IEEE Trans. Plasma Sci. **PS-19**, 286 (1991).

[9] K. Mittag, P. Choi, and Y. Kaufman, Nucl. Instrum. Methods Phys. Res. A **292**, 465 (1990).

[10] H. Pak and M. J. Kushner, J. Appl. Phys. **66**, 2325 (1989).

[11] H. Pak and M. J. Kushner, Appl. Phys. Lett. **57**, 1619 (1990).

[12] R. A. Petr, S. R. Byron, J. S. Demboski, J. J. Ewing, and M. J. Kushner, in *Digest of Technical Papers 5th IEEE Pulsed Power Conference*, edited by P. J. Tuichi and M. F. Rose (IEEE, New York, 1985), pp. 227–230.

[13] S. Lin and J. N. Bardsley, J. Chem. Phys. **66**, 435 (1977).

[14] C. B. Opal, W. K. Petersen, and E. C. Beatty, J. Chem. Phys. **55**, 4100 (1971).

[15] M. Hayashi, Nagoya Institute of Technology Report IPPJ-AM-19 (1981).

[16] D. Rapp and P. Englander-Golden, J. Chem. Phys. **43**, 1464 (1965).

[17] J. P. Boeuf and E. Marode, J. Phys. D **15**, 2169 (1982); electronic excitation cross sections were extrapolated to higher energies using analytic expressions.

[18] M. J. Schonhuber, IEEE Trans. Power Appar. Syst. **PAS-88**, 100 (1969).

[19] C. G. Morgan, in *Electrical Breakdown in Gases*, edited by J. M. Meek and J. D. Craggs (Wiley, Norwich, 1978), Chap. 7.